Reproductive ecology studies for sustainable fisheries management in Iberoamerica.
M. Bezerra Figueiredo, R. Domínguez-Petit, G. Macchi, R. Lessa, M.A. Perera, G. Plaza and S. Garrido (Eds)

Scientia Marina 89 (4)
December 2025, e111, Barcelona (Spain)
ISSN-L: 0214-8358
https://doi.org/10.3989/scimar.05639.111

Reproduction and growth of *Notacanthus bonaparte* (shortfin spiny eel): insights into the life history of a deep-sea species in the NE Atlantic

Sonia Rábade Uberos [1], Rosario Domínguez-Petit [2], Mariña Fabeiro [1], Juan Manuel Martínez Vázquez [3], Francisco Baldó [4], Rafael Bañón [5]

[1] Instituto de Investigaciones Marinas, (IIM-CSIC), Calle Eduardo Cabello 6, 36208 Vigo, Spain.
(SRU) (Corresponding autor) E-mail: soniaru@iim.csic.es. ORCID-iD: https://orcid.org/0000-0001-9914-7165
(MF) E-mail: fabeiro@iim.csic.es ORCID-iD: https://orcid.org/0000-0003-1120-6322
[2] Centro Oceanográfico de Vigo, Instituto Español de Oceanografía (IEO, CSIC), Subida a Radiofaro, 50, 36390 Vigo, Spain.
(RD-P) E-mail: rosario.dominguez@ieo.csic.es. ORCID-iD: https://orcid.org/0000-0003-1731-6848
[3] Centro Oceanográfico de Santander (COST-IEO) Planta de Cultivos Marinos el Bocal, Barrio Corbanera s/n 39012-Monte, Cantabria. Spain.
(JMMV) E-mail: jmauel.martinez@ieo.csic.es ORCID-iD: https://orcid.org/0000-0002-8923-4596
[4] Centro Oceanográfico de Cádiz (COCAD-IEO-CSIC), Puerto Pesquero, Muelle de Levante s/n, 11006 Cádiz, Spain.
(FB) E-mail: francisco.baldo@ieo.csic.es ORCID-iD: https://orcid.org/0000-0003-4220-4207
[5] Grupo de Estudo do Medio Mariño (GEMM), Edif. Club Náutico bajo, 15960 Ribeira, Spain.
(RB) E-mail: anoplogaster@yahoo.es ORCID-iD:https://orcid.org/0000-0001-6038-9335

Summary: This study investigates the reproductive biology and growth of *Notacanthus bonaparte* based on 158 specimens collected in October 2023 from the Porcupine area, NE Atlantic. The specimens measured between 172 and 495 mm total length. Sagitta otoliths were extracted, photographed, measured and sectioned, revealing age estimates ranging from 4 to 20 years. The growth rate coefficient (k) was calculated as 0.05±0.02 (1 year^{-1}). Gonads were dissected and analysed histologically, confirming that *Notacanthus bonaparte* in the NE Atlantic is an iteroparous species with group-synchronous oocyte development. Length at maturity (L_{50}) was estimated to be 280 mm of total length for both sexes combined. The parameters of the length-weight equation were *a*=15.15 and *b*=3.32, indicating positive allometric growth. This study offers new insights into the life history of *Notacanthus bonaparte* and provides valuable information on the population dynamics of this deep-sea species.

Keywords: Notacanthidae; maturity; reproduction; age reading; Porcupine Bank; deep sea.

Reproducción y crecimiento de *Notacanthus bonaparte* (anguila espinosa de aleta corta): claves sobre la historia de vida de una especie de aguas profundas en el Atlántico NE

Resumen: Este estudio investiga la biología reproductiva y el crecimiento de *Notacanthus bonaparte* a partir de 158 especímenes recogidos en octubre de 2023 en el área de Porcupine, Atlántico Nororiental. Los especímenes midieron entre 172 y 495 mm de longitud total. Los otolitos sagitales fueron extraídos, fotografiados, medidos y seccionados, revelando estimaciones de edad que oscilan entre 4 y 20 años. El coeficiente de la tasa de crecimiento (k) se calculó en 0.05±0.02 (1 año^{-1}). Las gónadas fueron extraídas y analizadas histológicamente, lo que confirmó que *Notacanthus bonaparte* en el Atlántico Nororiental es una especie iterópara con desarrollo de ovocitos sincrónico por grupos. La longitud de madurez (L_{50}) se estimó en 280 mm de longitud total para ambos sexos combinados. Los parámetros de la ecuación de longitud-peso fueron *a*=15.15 y *b*=3.32, lo que indica un crecimiento alométrico positivo. Este estudio ofrece nuevas perspectivas sobre la historia de vida de *Notacanthus bonaparte* y proporciona información valiosa sobre la dinámica poblacional de esta especie de aguas profundas.

Palabras clave: Notacanthidae; madurez; reproducción; lectura de edad; Banco de Porcupine; aguas profundas.

Citation/Como citar este artículo: Rábade Uberos S., Domínguez-Petit R., Fabeiro M., Martínez Vázquez J.M., Baldó F., Bañón R. 2025. Reproduction and growth of *Notacanthus bonaparte* (shortfin spiny eel): insights into the life history of a deep-sea species in the NE Atlantic. In: M. Bezerra Figueiredo et al. (Eds), Reproductive ecology studies for sustainable fisheries management in Iberoamerica. Sci. Mar. 89(4): e111. https://doi.org/10.3989/scimar.05639.111

Editor: G.J. Macchi, M. Bezerra Figueiredo.

Received: April 3, 2025. **Accepted:** June 17, 2025. **Published:** xxxx, 2025.

INTRODUCTION

The deep-sea ecosystem, extending from depths of 200 to 11000 m, encompasses over 65% of the Earth's surface, making it the planet's largest and least explored biome. Despite its vastness, the biological composition and ecological dynamics of deep-sea communities remain poorly understood. This knowledge gap is particularly concerning given the increasing anthropogenic pressures on deep-sea fish populations, which are often subject to exploitation without sufficient scientific data to inform conservation and management strategies.

The Porcupine Bank, located approximately 200 km west of Ireland on the Irish continental shelf, is a key area for deep-sea research in the Northeast Atlantic. Its bathymetry is complex: the northwestern margin is characterized by steep cliffs descending to depths of 1000 m, while the southeastern flank slopes gently into the Porcupine Sea Bight, accumulating significant sediment deposits (Velasco et al. 2008). The region is influenced by distinct water masses, including the northward-flowing Eastern North Atlantic Waters at 200–700 m, the Mediterranean Outflow Water at 800–1000 m, and the southward-flowing Labrador Sea Water at approximately 1100 m (O'Reilly et al. 2022).

The genus *Notacanthus* Bloch, 1788 comprises deep-water benthopelagic fishes with anguilliform bodies and distinctive short dorsal spines, whose number varies among species. Members of the family Notacanthidae inhabit depths ranging from 125 to 4900 m, with *Notacanthus* species typically occurring along the continental slope and lower rise between 125 and 3500 m (Bañón et al. 2024). Currently, the genus includes eight valid species, although the taxonomic status of *Notacanthus laccadiviensis* remains under debate (Bañón et al. 2024) and *Notacanthus chemnitzii* is considered a species complex pending further revision (Poulsen et al. 2018).

Three species are distributed in the Northeast Atlantic and Mediterranean Sea: *Notacanthus bonaparte* Risso, 1840; *Notacanthus arrontei* Bañón et al., 2024; and *Notacanthus chemnitzii* Bloch, 1788. The shortfin spiny eel, *N. bonaparte*, is distributed from the Faroe Islands to Mauritania, including the Western Mediterranean, at depths ranging from 487 to 2000 m (Mytilineou et al. 2005). Recent DNA barcoding studies suggest its presence may extend to Australian waters (Bañón et al. 2024).

Deep-sea fishes exhibit life-history traits such as late sexual maturation, slow growth, low fecundity and long lifespans, which render them particularly susceptible to environmental disturbances and overexploitation (Devine et al. 2006). Despite the ecological importance of these species, which often occupy mid- to upper trophic levels (Romeu et al. 2016), many of them remain poorly studied due to their limited commercial value and the logistical challenges of deep-sea research. The decline of these species could have cascading effects on deep-sea food webs and ecosystem functioning (Koslow et al. 2000).

Understanding the population dynamics of *N. bonaparte* in the Porcupine Bank is essential for generating baseline biological data to support ecosystem-based management of deep-sea fish stocks. While the species is currently listed as "Least Concern" in the Mediterranean (Papakonstantinou et al. 2011), its conservation status in the Atlantic remains unassessed, highlighting the need for region-specific data.

This study aims to enhance the biological knowledge of *N. bonaparte* in the Northeast Atlantic by estimating key life-history parameters—including length at maturity, length-weight relationships, growth metrics and fecundity—based on specimens collected from the Porcupine Bank.

MATERIALS AND METHODS

Sampling

A total of 158 individuals of *Notacanthus bonaparte* were collected in 21 bottom trawl hauls during a scientific survey conducted in September–October 2023 in the Porcupine Bank area (west of Ireland). The survey was carried out aboard the research vessel 'Vizconde de Eza' (Porcupine 2023, Spanish Oceanographic Institute, IEO-CSIC). Figure 1 shows the locations of the hauls where *N. bonaparte* was captured, at bottom depths ranging from 405 to 1473 m.

Specimens were identified taxonomically on board and biological sampling was then carried out. Fish were measured (total length, TL, mm), weighed (total and gutted weight, TW and GW, in g) and the sex of each individual was identified before extraction of gonads. Gonads were preserved in 3.6% buffered formaldehyde for further histological analysis. Otoliths were extracted and stored.

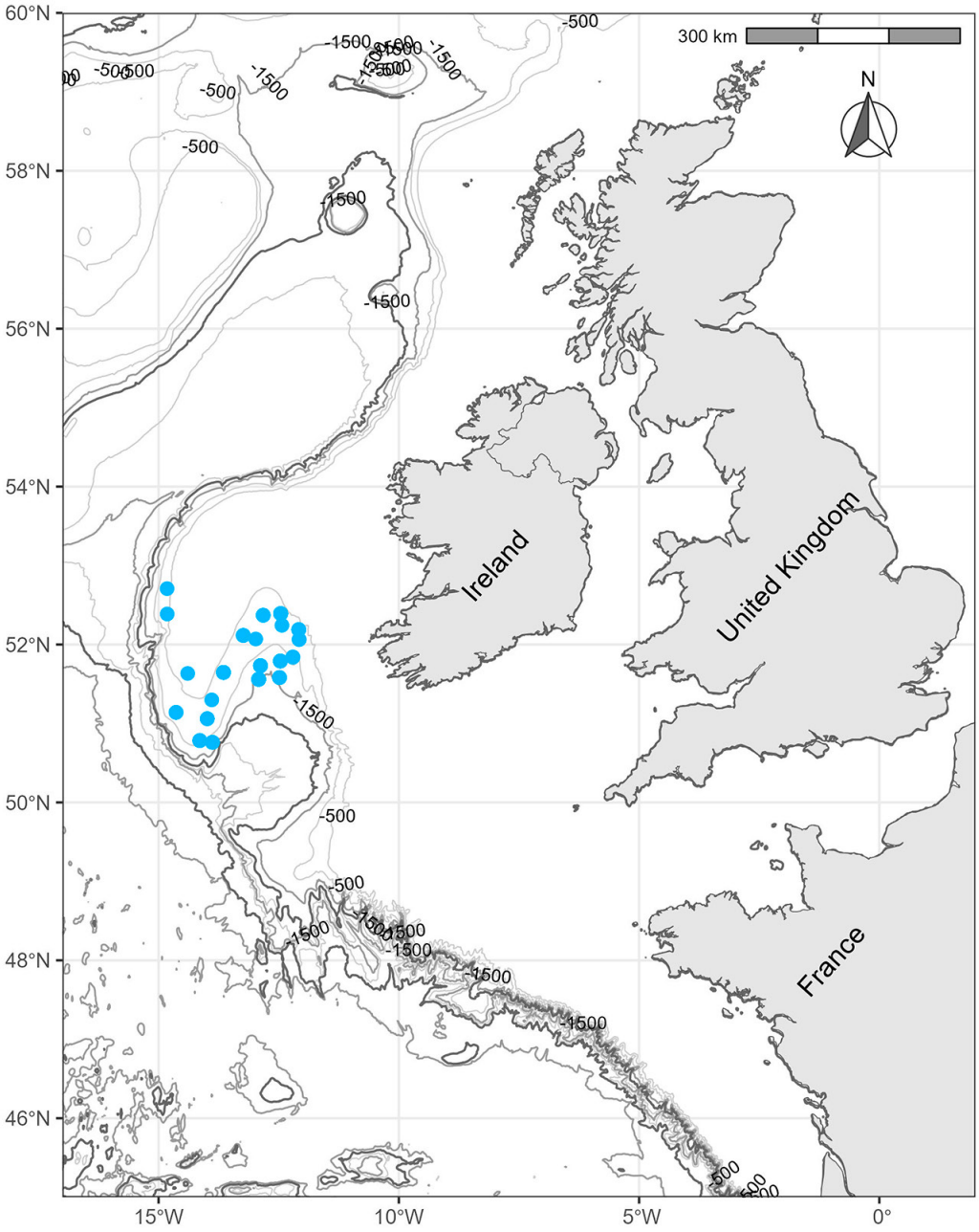

Fig. 1. – Map showing the hauls positive for *N. bonaparte* in the Porcupine 2023 survey.

Body size

Length and weight distributions among sexes were tested for differences using a Wilcoxon-test (*stats* package, R Core Team 2022)

Length-Weight relationship

To explore the length-weight relationship, the variables were log-transformed and logTL and logTW were fitted to the equation log TW=log *a*+*b* log TL, where *a* and *b* are the intercept and slope, respectively (Le Cren, 1951; Tesch, 1968).

We tested the hypothesis of isometric (h_0: b=3) or allometric growth (h_1: b≠3) using the *t*-tests implemented in the *hoCoef* function of the *FSAmisc* R package (Ogle 2022). We also calculated 95% confidence intervals for *b* and *a* of the linear model using the FSA R package (Ogle 2015).

Otoliths

Measurements

The sagitta otoliths of *N. bonaparte* (Fig. 2, left) are extremely small (maximum width 2.2 mm). We successfully extracted at least one sagitta otolith from 135 of the 158 individuals sampled on board. However, otoliths from only 121 individuals were measured, as the remaining ones either broke during extraction or exhibited crystallization or shape anomalies. The otoliths were photographed (sulcus acusticus upwards) and weighed (to the nearest 0.01 mg). Otoliths from the images were measured using an image analysis macro (Schindelin et al. 2012) to obtain height (anterior-posterior length, OH, µm), width (dorsal-ventral length, OW, µm), perimeter (P, µm) and area (A, µm^2). Otolith shape indices were also calculated: circularity (P^2/A), rectangularity ($A/(OH \times OW)$), aspect ratio (OW/OH; %) and OH/fish size.

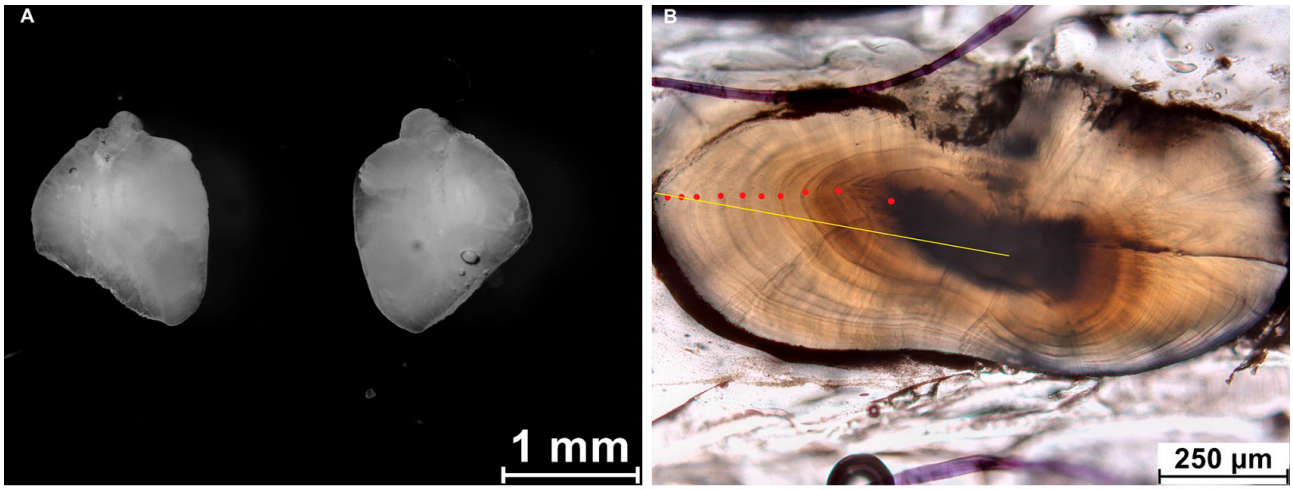

Fig. 2. – Pair of sagitta otoliths (A) and transverse section of an otolith (B) from a male measuring 350 mm TL.

Age reading

The otoliths were initially examined under a binocular microscope with incident light, but no ring patterns were distinguishable. A selection of 66 otoliths, preferably left-side otoliths, were then mounted on a crystal slide using transparent resin (Crystalbond™) and manually sanded with a grinding paper (diamond lapping film, 3, 1 and 0.5 microns). The otoliths were stuck on the crystal slide at the anterior end and ground until the nucleus was visible, then turned around and ground again to obtain a thin section. The thin sections of the otoliths (Fig. 2B) inspected under microscope showed an alternation of opaque and translucent bands that were quite contrasted. We considered the combination of one opaque and one translucent band to be an annual ring. After processing, the otoliths were photographed under microscope and ring interpretation was attempted by one reader (Fig. 2B). All otoliths were read three times by an expert reader and then compared with the results of an independent second reader. The edge was translucent in all specimens; thus, according to the criteria established in the ICES Workshop on age of deep-sea species (ICES, 2018), for specimens caught during the second half of the year, the age group assigned should be the previous (n–1) of the number of complete annual rings (n). The results were discussed, and in all cases the reading differences after discussion were less than 3 years between readers; the criterion of the expert reader was selected for further analysis.

Asymptote length (L_∞) and growth coefficient (k), were calculated from the von Bertalanffy equation.

Reproduction

Histology

The gonads were weighed after fixation using a precision scale (GnW, 0.001 g). A small piece of each gonad was processed histologically, dehydrated in ethanol, cleared in Histoclear™ and embedded in paraffin. The paraffin blocks were sectioned at 3–4 µm and stained with haematoxylin and eosin. Every preparation was examined under a microscope, sexed and assessed for gonadal developmental stage and fish maturity.

Ovary dynamics

During the microscopic inspection, the gonads were classified according to the developmental stage of the most advanced oocyte cohort (Tyler and Sumpter 1996). We applied the standardized terminology for males and females (Lowerre-Barbieri et al. 2023): immature (i), early-developing (ed), late-developing (ld), spawning (s), regressing (rg) and regenerating (rn).

To determine the type of oocyte development (synchronous or asynchronous) and spawning strategy (total or partial), we also measured the diameter of the oocytes in 12 females in the developing phase. Oocyte diameters were measured to the nearest 0.001 mm using the STERapp image analysis software (Mbaidin et al. 2021) with five to seven images for each female. This software recognizes whether the oocytes have a visible nucleus in the image, as only these oocytes are useful for determining the maximum diameter of each stage. The software enables the classification of the developmental stage of every oocyte in each image, which can be done manually (with human supervision) or automatically (after computer training).

In relation to oocyte measurements from histological images, we have to assume some bias in the diameters due to alterations (usually shrinkage) induced in the tissue by the histological processing, especially in the case of paraffin embedding (Saber et al. 2015). In this regard, it is recommended to interpret these data with caution. However, the primary objective of this analysis was to establish the developmental dynamics, which is not influenced by the histological procedure.

Size and age at maturity

Individuals were classified as mature or immature after microscopic inspection of the gonads according to Lowerre-Barbieri et al. (2023). Maturity data from 145 individuals were used to estimate the length and age at which there is a 50% probability of an individual being mature (L_{50} and A_{50}). To achieve this, a generalized linear model (McCullagh and Nelder, 1989) with a Bernoulli distribution (link logit) was applied, with maturity as the response variable and TL or age as the explanatory variables. Age and length at 50% maturity was estimated using the stats and sizeMat R packages (Torrejon-Magallanes, 2020; R Core Team, 2022). The variables are fitted to a logit function. L_{50} and A_{50} are then calculated as

$$P_{TL\ or\ A} = \frac{1}{1 + e^{-(\widehat{\beta 0} + \widehat{\beta 1} * X)}}$$

where P_{TL} or P_A are the probability of an individual being mature at a given length/age X. β_0 (intercept) and β_1 (slope) are the estimated parameters.

Fecundity

For the fecundity estimates, we analysed 31 females in the developing stage, weighed a subsample of the ovary (approximately 100 mg) and sifted through a sequence of sieves with mesh sizes ranging from 150 to 600 µm, aided by a jet of water spray to separate the oocytes from each other and from connective tissue. Images of the oocytes were taken under a binocular stereoscope, and later measured and counted using an image analysis macro (Schindelin et al. 2012).

Fecundity was calculated by counting and measuring all the oocytes in the ovary subsample with a mean diameter larger than 300 microns, which corresponds to the mean diameter of the oocytes at the secondary growth stage (previously calculated from histological sections) (Murua et al. 2003). The number of vitellogenic oocytes was then multiplied by the weight of the fixed ovary to obtain the total number of mature oocytes per ovary, the potential fecundity (F).

The relationship between fecundity and fish length was calculated using the formula $F=aTL^b$, (F: fecundity, TL: total length of the fish; a and b, constants) (Holden, 1974). We used a general linear model to test the relationship of fecundity with weight (eviscerated) and age.

Mean diameters of the secondary growth oocytes (>150 microns) were plotted against oocyte density in each ovary to calculate the autodiametric curve (Thorsen and Kjesbu 2001).

Patterns of vertical distribution

To investigate the existence of sexual segregation, we performed a linear regression to test for a correlation between sex, capture depth and TL, using TL as the response variable with sex and depth as covariates. The model assumptions were verified by plotting the residuals against the fitted values and each covariate in the model. The *stats* R package (R Core Team, 2022) was used to fit the model.

To explore the relation between the maturity phase of *N. bonaparte* and the depth of capture, we conducted a generalized linear model (McCullagh and Nelder 1989) with a Bernoulli distribution (link logit), with maturity as the response variable and depth and sex as explanatory variables, also testing for the interaction between depth and sex. The model assumptions were verified by plotting the residuals against the fitted values and each covariate in the model. Model selection was based on the Akaike information criterion. The *stats* R package (R Core Team, 2022) was used to fit the model.

RESULTS

Body size and length-weight relationship

The analysed specimens exhibited TLs ranging from 172 to 495 mm, with a mean of 364.8±60.8 mm (Fig. 3A). The smallest individuals, measuring 172 and 177 mm, could not be sexed due to unidentifiable gonads. On average, females were larger (mean=384.5 mm, sd=58.8 mm) than males (mean=343.2 mm, sd=35.8 mm). The smallest mature individuals measured 243 mm in both sexes, while the largest female reached 495 mm and the largest male 423 mm. Although the length distributions of males and females overlapped, females exhibited a wider range and higher modal values (Fig. 3A). In terms of weight, both sexes shared the same mode; however, females more frequently reached higher weights (Fig. 3B, C). Statistically significant differences in both length and weight were observed between sexes ($p<0.001$), while the differences in the length-weight relationship were marginally significant ($p<0.1$; Fig. 3C). As a result, a combined length-weight model was applied, producing coefficients of a=-15.1 and b=3.3, with a strong fit to the data ($R^2=0.94$).

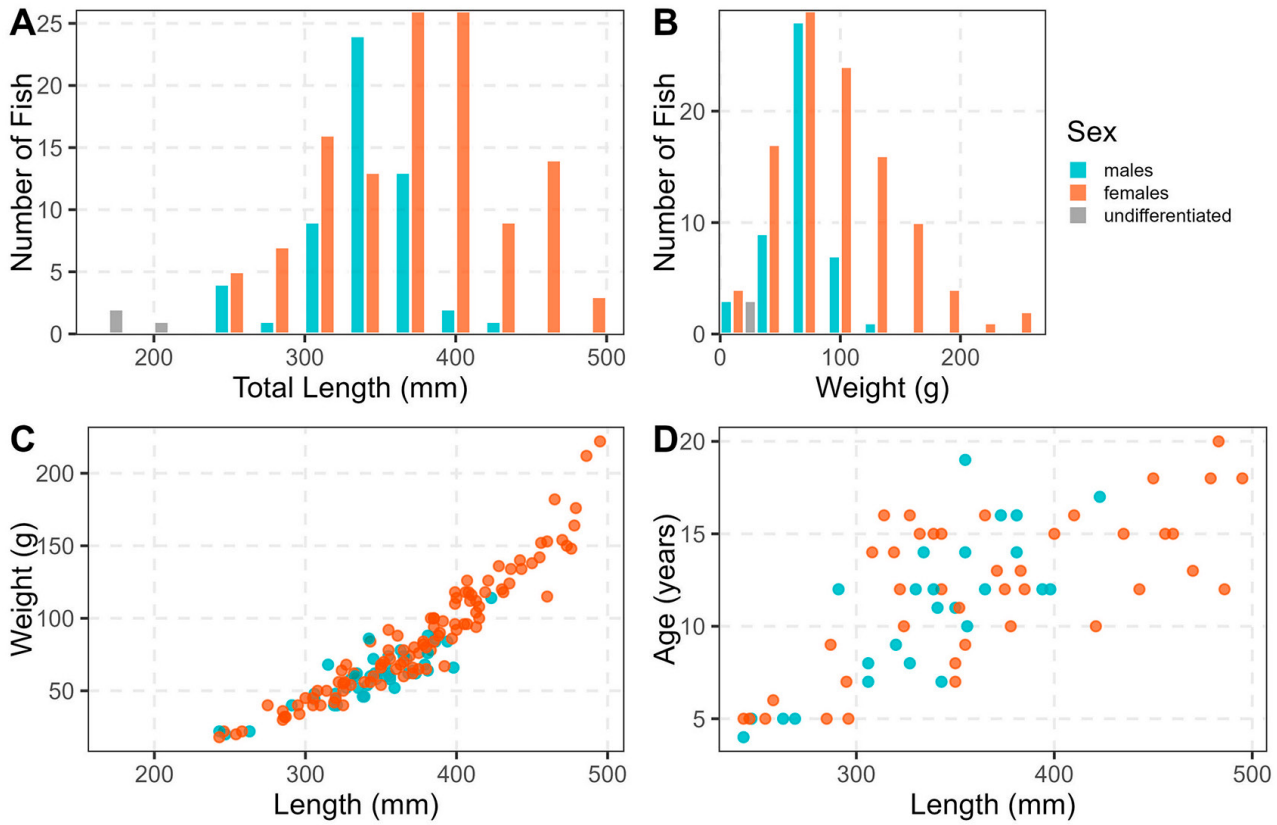

Fig. 3. – Frequency distribution of length (A) and gutted weight (B) by sex. Length-weight relationship (C) and age-length relationship (D) by sex in the sampled population of *N. bonaparte*.

Otolith morphology and age estimation

The sagitta otoliths were characterized as oval, bi-convex and nodular, featuring a distinct arrow-shaped anterior edge and a rounded posterior margin (Fig. 2, left). The otolith dimensions—including height, width, area, and perimeter (Table 1)—were significantly correlated with fish total length ($p<0.001$) and sex ($p<0.05$), with females

exhibiting more pronounced growth. In contrast, shape descriptors such as circularity, rectangularity and aspect ratio showed no significant associations with either variable.

The first annulus was defined as a dark region adjacent to the nucleus, consistently observed across all specimens, with a mean distance from the core of 313±36 µm. Female ages ranged from 4 to 20 years while males ranged from 4 to 19 years. Growth patterns were described using the von Bertalanffy growth function. Sex-specific models could not be fitted because the female model failed to converge. The combined-sex model yielded the following parameters: asymptotic length Lα=631 mm (bootstrap sd=61.5 mm) and growth coefficient k=0.05, with a 95% bootstrap confidence interval of [0.05,0.13].

Table 1. – Mean values of otolith measurements (microns) and weight (mg).

Sex	Males		Females		Total
Otolith	Left	Right	Left	Right	Mean
Area (µm^2)	1394600	1381557	1587254	1598098	1518439
Perimeter	4996	5190	5328	5719	5369
Width	1260	1262	1356	1357	1322
Height	1506	1501	1569	1592	1552
Circularity	18.4	20.1	18.4	21.4	19.7
Rectangularity	0.73	0.72	0.73	0.72	0.72
Aspect ratio	83.9	84.2	86.5	84.6	85.0
Weight	1.30	1.35	1.56	1.61	1.49

Reproductive maturity and gonadal development

Macroscopically, immature ovaries appeared white and flat, while mature ones were yellowish, elongated and folded. The oocytes within the germinal epithelium were arranged in parallel lamellae, and the absence of an ovarian lumen suggests that mature oocytes are released directly into the peritoneal cavity. Testes were small, flat and whitish.

Microscopic examination identified 15 immature gonads, comprising 10 females (Fig. 4A) with lengths ranging from 243 to 296 mm and 5 males (Fig. 4E) with lengths ranging from 263 to 381 mm. The majority of specimens were classified as mature. Among mature females, 80 were in the developing phase (Fig. 4B,C,D) and 3 in the regenerating phase. Most males were also in the developing phase (n=45), characterized by the presence of spermatogonia and primary spermatocytes (Fig. 4F). Additionally, five males were in the spawning phase, exhibiting all spermatogenic stages, including spermatozoa (Fig. 4G).

Oocytes were observed in primary growth (96±21 µm), cortical alveoli (148±16 µm) and vitellogenesis (317±70 µm) (Fig. 4B,C). A threshold of 130 µm was proposed to distinguish primary from secondary growth. Clear postovulatory follicles (POFs) were found in one spawning female (TL=413 mm, Fig. 4D), suggesting that *N. bonaparte* is a batch spawner. Furthermore, another female in the regenerating phase showed recent POFs, while other females had structures compatible with degrading POFs.

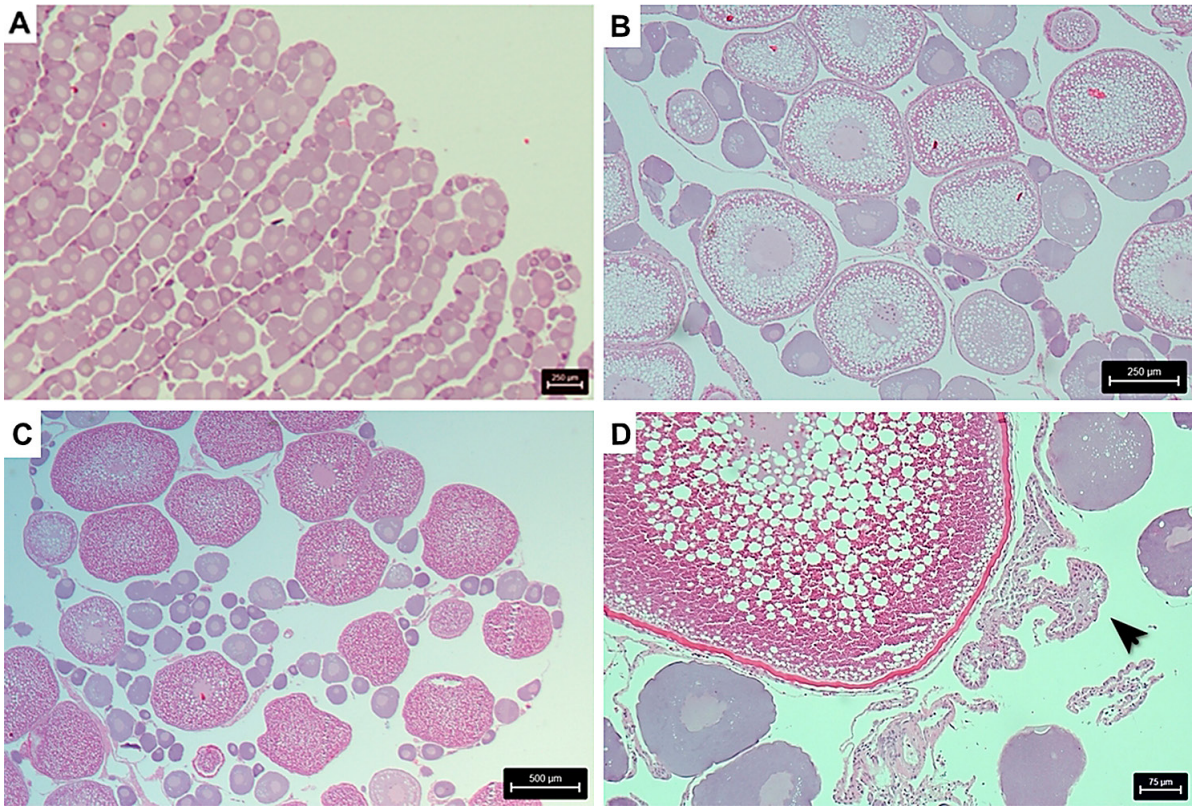

Fig. 4. – Maturity stages of ovaries (A–D) and testes (E–F) of *N. bonaparte*: A, immature; B, early vitellogenic; C, mid-late vitellogenic; D, postovulatory follicles; E, immature; F, developing.

Maturity ogive

Due to the low number of immature males, a combined-sex logistic model was used. We estimated size and age at 50% maturity:

L_{50}=280 mm, (a=-11.13, b=0.04, R^2=0.47), (Fig. 5A).
A_{50}=5.6 years, (a=-1.72, b=0.31, R^2= 0.29), (Fig. 5B).

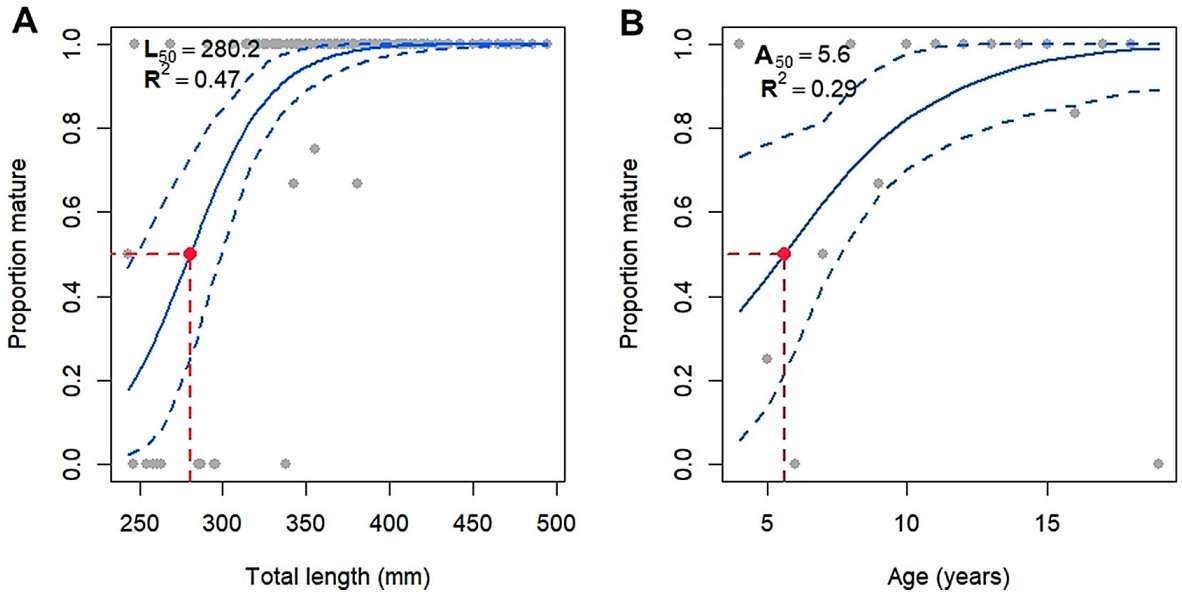

Fig. 5. – Fitted curve of the probability of maturity at length (A) and age (B).

Ovary dynamics and fecundity

Oocyte size frequency distribution revealed two distinct cohorts in secondary growth—cortical alveoli and vitellogenesis—that became increasingly separated as maturation progressed. The most advanced cohort, corresponding to early-to-late vitellogenesis, exhibited a broad unimodal distribution ranging from 177 to 585 µm (Fig. 6).

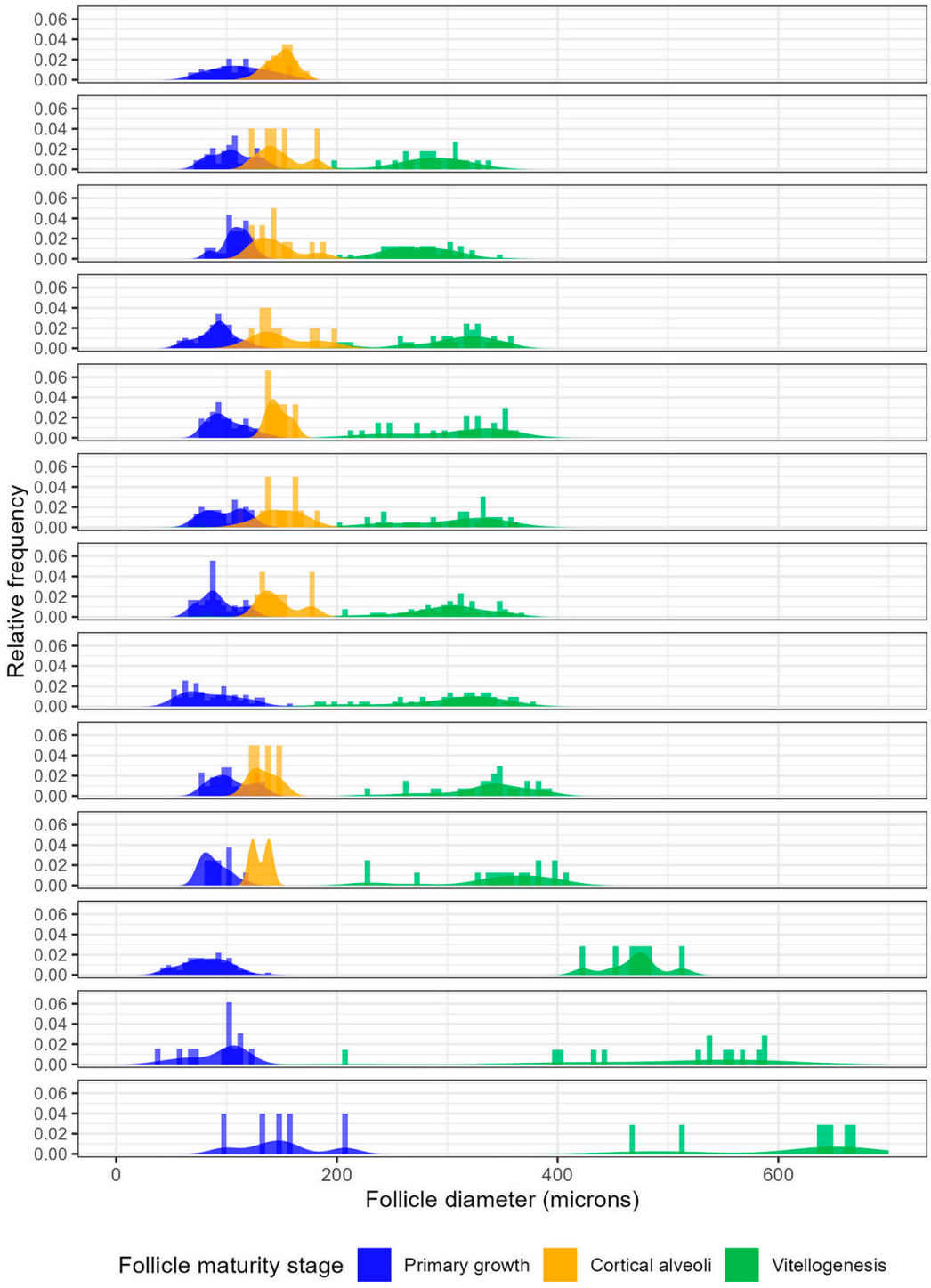

Fig. 6. – Oocyte diameter distribution in females of *N. bonaparte*.

Quantitative analysis showed that 56% of the oocytes were in primary growth, 14% in the cortical alveoli stage, and 30% in vitellogenesis. In ovaries at advanced vitellogenesis, the proportion of primary growth oocytes increased to 81%.

Total fecundity, estimated from oocytes in secondary growth, ranged from 4823 to 45223 oocytes, with a mean of 19474±9463. Oocyte density varied between 720 and 6649 oocytes per gram of ovary. Oocytes in the cortical alveoli stage represented less than 2% of total fecundity.

The autodiametric fecundity curve was best described by a polynomial equation (Fig. 7A). Fecundity showed a significant positive relationship with female length ($p<0.1$), modelled by a power function ($a=158.31$; $b=1.29$), which explained 11% of the variance (Fig. 7B). No significant relationship was found between fecundity and either body weight or age.

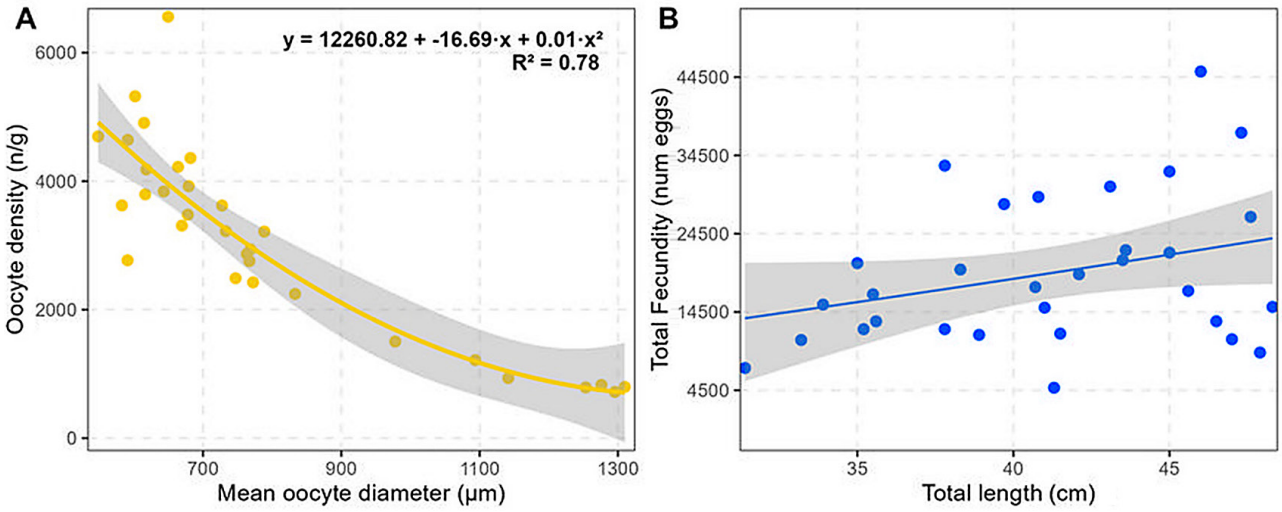

Fig. 7. – (A) autodiametric fitting curve; (B) fit of the relationship between fecundity and female total length.

Vertical distribution patterns

Length and depth

Fish length was significantly influenced by both sex and depth ($p<0.001$; Fig. 8, Table 2), though their interaction was not significant. Females were generally larger and found at greater depths. These two factors explained 25% of the variance in length.

Table 2. – Results of the linear models fitting fish length and maturity as a function of depth and sex.

		Estimate	Standard error	p-value
Total length	Intercept	389.85	11.46	<0.001
	Depth	–0.06	0.01	<0.001
	Sex(F)	54.63	8.59	<0.001
Maturity	Intercept	3.65	0.89	<0.001
	Depth	–0.005	0.0008	<0.05
	Sex(F)	0.16	0.61	

Maturity and depth

Immature males were found at shallower depths (mean=625 m) than mature males (770 m), while immature females were found deeper (1260 m) than mature ones (929 m). Spawning males were only found in the deepest haul (1473 m), though sample size was limited (n=5). Developing females had a broader vertical distribution than males.

Maturity was significantly correlated with depth ($p<0.05$), but not with sex. However, the model explained only 4% of the variance (Fig. 8, Table 2).

Of the morphological traits analysed, body size and otolith dimensions were positively associated with depth. Larger individuals, particularly females, tended to inhabit deeper waters. This suggests a potential ecological adaptation linking morphology to vertical distribution in *N. bonaparte.*

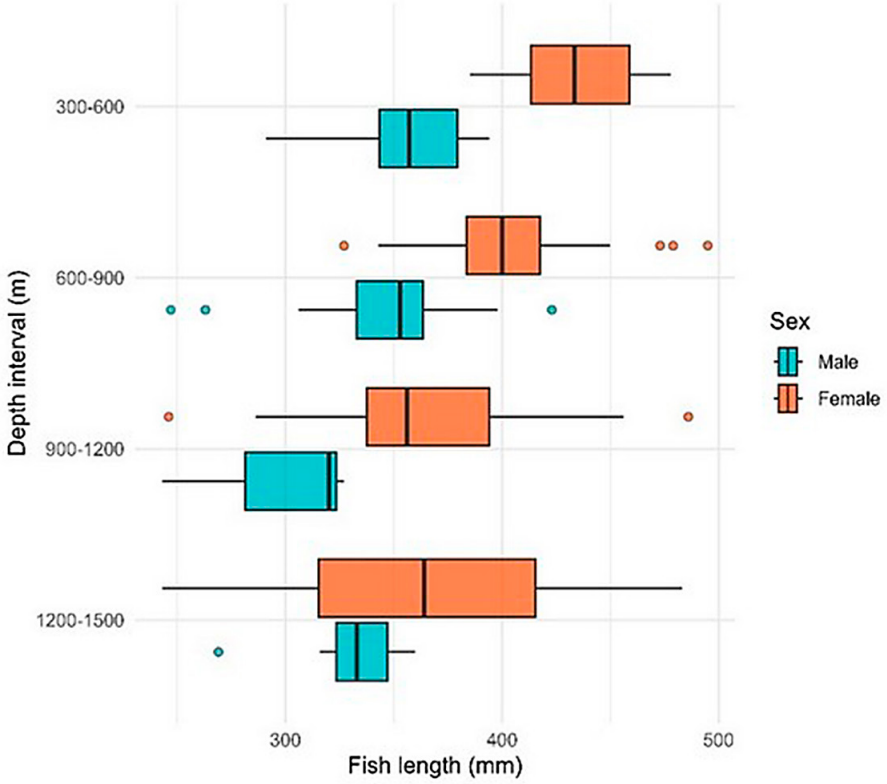

Fig. 8. – Vertical distribution of *N. bonaparte* by sex and length.

DISCUSSION

Growth patterns: length and weight

The results confirm sexual dimorphism in *N. bonaparte*, with females being significantly larger and heavier than males. The length-weight relationship showed marginally significant differences between sexes ($p<0.1$; Fig. 3C), suggesting different energy allocation strategies. The combined length–weight model demonstrated positive allometric growth ($b=3.3$, $R^2=0.94$), validating its applicability for estimating weight from length in population studies. This sexual dimorphism with larger females is consistent with observations in other populations of *N. bonaparte* in the Porcupine Seabight, although this difference was not significant in the Rockall Trough (Coggan et al. 1997). These findings suggest a life-history strategy in which females maximize fitness through larger body size, potentially linked to increased fecundity or survival advantages. The observed differences in growth patterns may possibly highlight sex-specific selective pressures within the species (Horne et al. 2020).

Growth patterns: otoliths and age

This study presents the first age data for *N. bonaparte*, with the oldest individual being a 20-year-old female measuring 483 mm in length. The maximum age previously reported for a Notacanthiforme was 26 years for *N. chemnitzii* (Vedishcheva et al. 2016). In all specimens, an intense dark area around the nucleus was observed, which

according to Vedishcheva et al. (2016) may correspond to the first annulus. Sexual dimorphism was detected in several otolith dimensions, including width, area, weight, height and perimeter, suggesting sex-specific differences in physiology and growth rate (Mille et al. 2015). Otolith width and area were identified as the most reliable predictors of fish length (R^2>0.7).

Deep-sea fish species like *N. bonaparte* are generally considered to be at the end of the K-selection life-history spectrum, characterized by slow growth, delayed maturity and a long lifespan (De Forges et al. 2000; Priede 2017). The von Bertalanffy growth equation for *N. bonaparte* indicated a slow growth rate (k=0.05). We captured the largest individual reported in the literature (495 mm TL), significantly exceeding previous records from the Mediterranean (285 mm TL) and the sub-Arctic Atlantic (399 mm TL). However, given the estimated growth curve (Fig. 9), it is likely that we have not yet captured the species' asymptotic size.

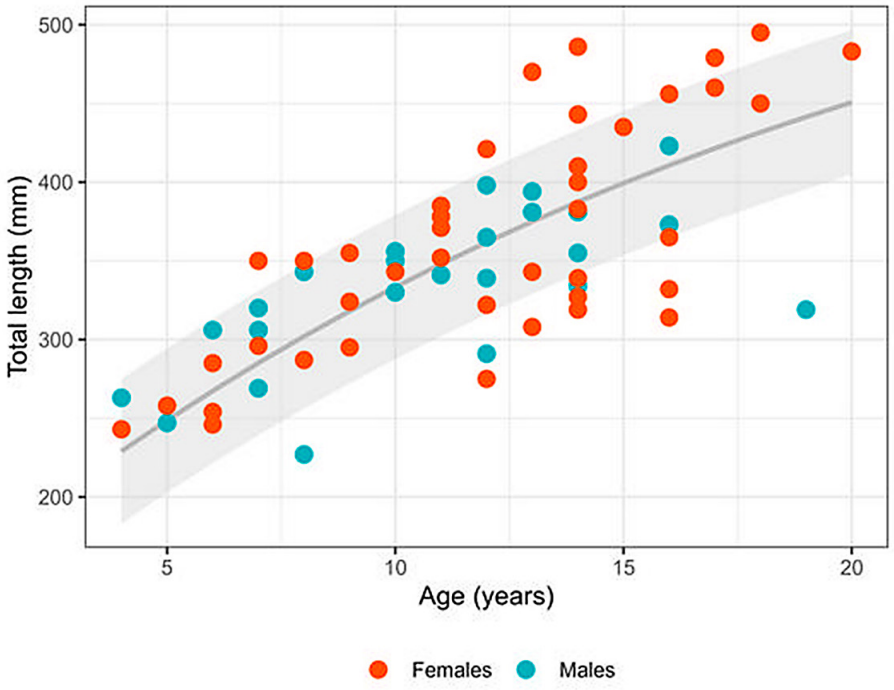

Fig. 9. – Fit of the von Bertalanffy's growth model.

Reproductive traits

We found undifferentiated gonads in individuals up to 180 mm, but from 243 mm all were sexually differentiated. Coggan et al. (1997) observed sexual differentiation occurring between 96 and 232 mm TL (40–100 mm gnatoproctal length). In our study, the smallest mature female and male measured, respectively, 275 and 227 mm TL.

Our estimates for the length at first maturity (L_{50}) and age at first maturity (A_{50}), combining both sexes, were 280 mm TL and 5.6 years, respectively. Previous studies in the Porcupine Seabight reported a size at first maturity for females of 216 mm TL (Coggan et al. 1998), but no prior data exist regarding the age at maturity for *N. bonaparte*. Direct comparisons with earlier findings are complicated by methodological differences, specifically, the use of macroscopic versus histological staging in maturity assessment. Such differences can lead to overestimation of size at maturity, as regenerating individuals may be misclassified as immature. In the Mediterranean, comparable studies indicated the onset of reproductive activity at 180–199 mm TL (Piscitelli et al. 1998). Given the nature of existing data, it is unclear whether the Porcupine Bank population is currently delaying reproduction or simply growing at a faster rate. Notably, differences between the Mediterranean and Porcupine Bank populations extend beyond length at first maturity and are evident across the entire size spectrum (Romeu, 2014).

The low number of immature males in our samples precluded sex-specific estimation of length at 50% maturity (L_{50}). However, as males typically mature at smaller sizes than females in sexually dimorphic fish species (Horne et al. 2020), their inclusion in our combined-sex L_{50} estimate would likely reduce the overall value.

L_{50} exhibits significant plasticity in response to environmental and population-level drivers, reflecting adaptive trade-offs between growth and maturation (Dieckmann and Heino 2007). Notably, delayed size at maturity does not inherently imply delayed *age* at maturity, as these traits respond independently to drivers such as fishing-induced selection, mortality, environmental conditions and population density. This plasticity may represent an adaptive strate-

gy to optimize reproductive success in slow-growing species, reflecting evolutionary responses to extreme deep-sea constraints. Long-term monitoring of L_{50} would thus provide critical data for future population assessments.

The presence in our samples of at least one female in advanced vitellogenesis with recent POFs strongly supports the hypothesis of batch spawning for this species. The contribution of the less advanced oocyte cohorts was 2%, a value similar to the 5% reported by Coggan et al. (1998). Such low percentages raise questions about the fate of these oocytes: whether they represent a residual cohort destined for reabsorption or a potential second cohort that would be released later in the reproductive season. The hiatus between secondary growth oocytes suggests that only the most advanced oocytes are recruited for spawning (Ganias et al. 2015). These observations indicate a group-synchronous ovarian development strategy. However, due to sampling limitations, we were unable to determine the number of batches released during the spawning season or its total duration.

Our estimate of the fecundity of *N. bonaparte* on the Porcupine Bank (mean=9474 eggs) falls within an intermediate range between previous values reported for the Atlantic (Coggan et al. 1998, 30600 eggs; Merrett 1994, 21540 eggs) and those documented for the Mediterranean (Piscitelli et al. 1998, 7322 eggs), reinforcing the existence of significant population-level differences between regions, as also observed for L_{50}.

Fecundity is a plastic trait that can be modulated by both environmental and anthropogenic factors, including fishing pressure and pollution (Bera et al. 2022; Taslima et al. 2022; Murua et al. 2003; Liu et al. 2024). Although microplastic concentrations in the area are elevated (Nash et al. 2023), levels of polycyclic aromatic hydrocarbons and trace metals in sediments remain low (Viñas et al. 2023), and thus the actual impact of pollution on fecundity requires further investigation. Our data suggest a possible decline in fecundity on the Porcupine Bank, although this trend should be confirmed by future sampling. Furthermore, our analyses indicate that body length has a limited influence on egg production, accounting for only 11% of observed variability, while neither weight nor age showed significant effects. These findings partially contrast with previous studies reporting an effect of weight (Coggan et al. 1998) or a lack of correlation with length (Piscitelli et al. 1998). Fecundity in fish is typically influenced by body size, and since body size generally increases with age, fecundity is often associated with age as well. In this study, fecundity was estimated in a limited number of individuals and across few age groups. This, combined with the overlap in size distributions within age classes, may mask any potential effect of age on fecundity. On the other hand, the weak relationship between length and fecundity may be attributed to the species' slow growth and late maturation, prioritizing survival over reproductive investment, or to additional factors not considered here, such as environmental conditions, hormonal influences or reproductive migrations (Murua et al. 2003). While the literature generally identifies length and condition as the main determinants of fecundity variability, the potential occurrence of reproductive migrations could mask this relationship in our study if sampling did not fully cover the entire size range of the population during the reproductive season.

The temporal coverage of our sampling does not permit a comprehensive description of the reproductive cycle of *N. bonaparte*; however, our results suggest that this species is iteroparous, displaying group-synchronous oocyte development and batch spawning.

For instance, an extended breeding season during summer has been reported in the Gulf of Genoa (Cabo, 1952), while the Ionian Sea is characterized by two short reproductive periods, from November to January and April to July (Piscitelli et al. 1998). In contrast, the northwestern Mediterranean shows year-round spawning with a peak in spring and summer (Fernandez-Arcaya et al. 2013), and in the Western Mediterranean, the reproductive season spans from late summer to autumn (Romeu et al. 2016). Although these studies also present limitations in spatial, seasonal or vertical coverage, the observed variability in spawning timing and duration underscores the adaptability of reproductive strategies, likely in response to environmental factors that shape deep-sea ecosystems (Milligan et al. 2020).

The benthopelagic environment is generally considered stable; for example, at depths of around 400 m in the Porcupine Basin, water temperature remains relatively constant at approximately 11°C throughout the year (Sangiorgi et al. 2021). However, processes such as water column stratification and mixing can disrupt this stability, influencing the vertical flux of organic matter and, consequently, the availability of food resources for prey species—primarily ophiuroids and sedentary coelenterates (Coggan et al. 1998; Romeu et al. 2016). These fluctuations in food supply may play a crucial role in modulating reproductive timing and success in *N. bonaparte*.

Vertical distribution

Our sampling revealed sexually undifferentiated individuals at ~1000 m depth, consistent with limited knowledge of notacanthid early life stages. These taxa exhibit leptocephalus larvae with pelagic phases potentially lasting ≤3 years (Harrisson, 1966). The sole documented *N. chemnitzii* larva in the Porcupine Seabight (197 mm TL at 655–680 m; Merrett 1981) suggests benthic transition precedes the juvenile stage. Vertical ontogenetic migration—a common phenomenon in deep-sea fishes (Nielsen et al. 1999) —is supported by otolith microchemistry (Chang et al. 2015). We observed a distinctive mark at ~300 µm from the core, aligning with the "juvenile growth mark" in *N. chemnitzii* (Vedishcheva et al. 2016) This implies similar migration in *N. bonaparte*, though the timing remains unresolved given evidence of benthic larval development (Merrett, 1981) and potential "prolonged infantilism" (≤3 years; Harrison 1966). Future studies should address these uncertainties in age estimation protocols.

The presence of females with recent POFs confirms active reproduction during sampling. However, low POF prevalence suggests incomplete coverage of spawning areas. Cold temperatures slow POF degradation (Kurita et al. 2011), potentially enhancing detection (Witthames et al. 2010). Coggan et al. (1998) documented winter-spring spawning in the Porcupine Seabight/Rockall Trough but captured few spawning females, hinting at unlocalized spawning grounds. Both our results and the available literature point to *N. bonaparte* spawning in deep areas that have not yet been adequately represented in sampling efforts.

Developing individuals were found throughout the sampled depth range, whereas immature females were mostly restricted to 1000–1500 m and immature males to 600–700 m. Most males (81%: immature and developing) occurred at 400–800 m, with the remainder (developing and spawning) found deeper, including at the maximum sampled depth of 1473 m, suggesting that males migrate downslope as they mature. Previous studies in the region found the highest abundance (formed by small, immature, individuals) located in the upper levels (Coggan et al. 1997, 1998) and the largest individuals (with a skewed sex ratio favouring females) at greater depths, with spawning females concentrated at 1000–1750 m—a range underrepresented in our survey. This likely explains the scarcity of spawning females and males with recent reproductive activity in our samples, indicating that we probably did not encompass the main spawning grounds or peak reproductive period. Depth-distribution patterns suggest that the Rockall Trough may function as a nursery, with juveniles migrating southward to the Porcupine Seabight via the Labrador Current.

As a specialized benthopelagic predator (Romeu, 2014, Romeu et al. 2016)), *N. bonaparte* plays a critical role in deep-sea food webs. Understanding its life history is essential for modelling deep-sea ecosystems, implementing ecosystem-based fisheries management (Farrag 2016; León-Cobo et al. 2023) and informing conservation strategies for poorly studied non-commercial species. This study underscores the value of fisheries survey data for revealing ecological insights. Future research requires comprehensive sampling across the Porcupine Bank, Rockall Trough and Porcupine Seabight to resolve reproductive complexities.

ACKNOWLEDGEMENTS

The authors wish to thank all participants in the PORCUPINE 2023 research cruise and the crew of the R/V *Vizconde de Eza* for their help during the sampling.

CONFLICTS OF INTEREST

The authors declare no conflict of interest. The funders had no role in the design of the study; in the collection, analyses or interpretation of data; in the writing of the manuscript; or in the decision to publish the results.

FUNDING SOURCES

The cruise was supported by the Instituto Español de Oceanografía (IEO) and by the Data Collection Framework for the EU Common Fisheries Policy.

AUTHORSHIP CONTRIBUTION STATEMENT

Sonia Rábade Uberos: conceptualization, formal analysis, data curation, investigation, methodology, visualization, writing – original draft, writing – review and editing. **Rosario Domínguez-Petit:** conceptualization, supervision, writing – review and editing. **Mariña Fabeiro:** resources. **Juan Manuel Martínez Vázquez:** resources. **Francisco Baldó:** funding acquisition, project administration, resources, supervision, writing – review and editing. **Rafael Bañón:** resources, writing – review and editing.

REFERENCES

Bañón R., Barros-García D., Baldó F., et al. 2024. Unveiling taxonomic diversity in the deep-sea fish genus *Notacanthus* (Notacanthiformes: Notacanthidae) with description of *Notacanthus arrontei* n. sp. J. Fish Biol. 104(6): 1910–1923. https://doi.org/10.1111/jfb.15734

Bera T., Kumar S. V., Devi M.S., et al. 2022. Effect of heavy metals in fish reproduction: A review. J. Environ. Biol. 43: 631–642. https://doi.org/10.22438/jeb/43/5/MRN-4042

Cabo F.L. 1952. Estudio preliminar sobre la biometría, la biología y la anatomía general de *Notacanthus bonapartei* Risso. Bol. del Inst. Español Oceanogr. 49.

Chang N.N., Liu E.Y., Liao Y.C., et al. 2015. Vertical habitat shift of viviparous and oviparous deep-sea cusk eels revealed by otolith microstructure and stable-isotope composition. J. Fish Biol. 86: 845–853. https://doi.org/10.1111/jfb.12605

Coggan R.A., Gordon J.D., Merrett N.R. 1997. Notacanthid fishes of the Rockall Trough and Porcupine Seabight, west of the British Isles. Biol. Behav. CMI997/BB:

Coggan R.A., Gordon J.D.M., Merrett N.R. 1998. Abundance, distribution, reproduction and diet of notacanthid fishes from the north-east Atlantic. J. Fish Biol. 52: 1038–1057. https://doi.org/10.1006/jfbi.1998.0650

De Forges B.R., Koslow J.A., Pooro G.C.B. 2000. Diversity and endemism of the benthic seamount fauna in the southwest Pacific. Nature 405: 944–947. https://doi.org/10.1038/35016066

Devine J.A., Baker K.D., Haedrich R.L. 2006. Deep-sea fishes qualify as endangered. Nature 439: 29. https://doi.org/10.1038/439029a

Dieckmann U., Heino M., 2007. Probabilistic maturation reaction norms: Their history, strengths, and limitations. Mar. Ecol. Prog. Ser. 335: 253–269. https://doi.org/10.3354/meps335253
Farrag M.M.S. 2016. Deep-sea ichthyofauna from Eastern Mediterranean Sea, Egypt: Update and new records. Egypt. J. Aquat. Res. 42: 479–489. https://doi.org/10.1016/j.ejar.2016.12.005
Fernandez-Arcaya U., Rotllant G., Ramirez-Llodra E. et al. 2013. Reproductive biology and recruitment of the deep-sea fish community from the NW Mediterranean continental margin. Prog. Oceanogr. 118: 222–234. https://doi.org/10.1016/j.pocean.2013.07.019
Ganias K., Lowerre-Barbieri S.K., Cooper W. 2015. Understanding the determinate-indeterminate fecundity dichotomy in fish populations using a temperature dependent oocyte growth model. J. Sea Res. 96: 1–10. https://doi.org/10.1016/j.seares.2014.10.018
Harrisson C.M.H. 1966. On the first Halosaur Leptocephalus from Madeira. Bull. Br. Museum natural Hist. Zool. 14: 441–486.
Holden M.J. 1974. Manual of fisheries science. Part 2 - Methods of resource investigation and their application. Food and Agriculture Organization (FAO), Rome.
Horne C.R., Hirst A.G., Atkinson D. 2020. Selection for increased male size predicts variation in sexual size dimorphism among fish species. Proc. R. Soc. B Biol. Sci. 287(1918): 20192640. https://doi.org/10.1098/rspb.2019.2640
ICES. 2018. Workshop on Age Estimation Methods of Deep-Water Species (WKAMDEEP2), 17 -21 September 2018, Cadiz, Spain. ICES CM 2018/EOSG:27.
Koslow J.A., Boehlert G.W., Gordon J.D.M. et al. 2000. Continental slope and deep-sea fisheries: Implications for a fragile ecosystem. ICES J. Mar. Sci. 57: 548–557. https://doi.org/10.1006/jmsc.2000.0722
Kurita Y., Fujinami Y., Amano M. 2011. The effect of temperature on the duration of spawning markers-migratory-nucleus and hydrated oocytes and postovulatory follicles- in the multiple-batch spawner Japanese flounder (*Paralichthys olivaceus*). Fish. Bull. 109: 79–89.
Le Cren E.D. 1951. The Length-Weight Relationship and Seasonal Cycle in Gonad Weight and Condition in the Perch (*Perca fluviatilis*). J. Anim. Ecol. 20: 201–219. https://doi.org/10.2307/1540
León-Cobo M.J., de Carvalho-Souza G., Cuesta J.A., et al. 2023. New records of the deep-sea fish species *Tetragonurus cuvieri* (Risso, 1810) and *Notacanthus bonaparte* (Risso, 1840) (Chordata: Teleostei) in Southwestern Europe (Gulf of Cádiz, SW Spain). ARPHA Prepr. e111930 https://doi.org/10.3897/arphapreprints.e111930
Liu H., Li H., Liu Y., et al. 2024. Toxic effects of microplastic and nanoplastic on the reproduction of teleost fish in aquatic environments. Environ. Sci. Pollut. Res. 31: 62530–62548. https://doi.org/10.1007/s11356-024-35434-9
Lowerre-Barbieri S.K., Nancy J. B.-P., Wyanski D.M., et al. 2023. A unified framework and terminology for reproductive traits integral to understanding fish population productivity. Mar. Coast. Fish. 15: 1–30. https://doi.org/10.1002/mcf2.10276
Mbaidin A., Rábade-Uberos S., Dominguez-Petit R., et al. 2021. Sterapp: Semiautomatic software for stereological analysis. application in the estimation of fish fecundity. Electronics 10: 1432. https://doi.org/10.3390/electronics10121432
McCullagh P., Nelder J.A. 1989. Generalized Linear Models, 2nd ed. Chapman and Hall, London, 526 pp.
Merrett N.R. 1981. First record of a notacanth leptocephalus; a benthopelagic capture in the slope waters off Ireland. J. Fish Biol. 18: 53–57. https://doi.org/10.1111/j.1095-8649.1981.tb03759.x
Merrett N.R. 1994. Reproduction in the North Atlantic oceanic ichthyofauna and the relationship between fecundity and species' sizes. Environ. Biol. Fishes 41: 207–245. https://doi.org/10.1007/BF00023814
Mille T., Mahe K., Villanueva M.C., et al. 2015. Sagittal otolith morphogenesis asymmetry in marine fishes. J. Fish Biol. 87: 646–663. https://doi.org/10.1111/jfb.12746
Milligan R.J., Scott E.M., Jones D.O.B., et al. 2020. Evidence for seasonal cycles in deep-sea fish abundances: A great migration in the deep SE Atlantic? J. Anim. Ecol. 89: 1593–1603. https://doi.org/10.1111/1365-2656.13215
Murua H., Kraus G., Saborido-Rey F., et al. 2003. Procedures to Estimate Fecundity of Marine Fish Species in Relation to their Reproductive Strategy. J. Northw. Alt. Fish. Sci. 33: 33–54. https://doi.org/10.2960/J.v33.a3
Mytilineou C., Politou C.Y., Papaconstantinou C., et al. 2005. Deep-water fish fauna in the Eastern Ionian Sea. Belgian J. Zool. 135: 229–233.
Nash R., Joyce H., Pagter E., et al. 2023. Deep Sea Microplastic Pollution Extends Out to Sediments in the Northeast Atlantic Ocean Margins. Environ. Sci. Technol. 57: 201–213. https://doi.org/10.1021/acs.est.2c05926
Nielsen J.G., Cohen D.M., Markle D.F., et al. 1999. Ophidiiform fishes of the world (Order Ophidiiformes). An annotated and illustrated catalogue of pearlfishes, cusk-eels, brotulas and other ophidiiform fishes known to date. FAO Fisher. ed, FAO Species Catalogue. FAO, Rome.
O'Reilly L., Fentimen R., Butschek F., et al. 2022. Environmental forcing by submarine canyons: Evidence between two closely situated cold-water coral mounds (Porcupine Bank Canyon and Western Porcupine Bank, NE Atlantic). Mar. Geol. 454: 106930. https://doi.org/10.1016/j.margeo.2022.106930
Ogle D. 2015. Introductory Fisheries Analyses with R. Chapman and Hall, New York, 337 pp. https://doi.org/10.1201/9781315371986
Ogle D. 2022. FSAmisc: Miscellaneous functions for simple fisheries stock assessment methods. R package version 0.0.3.
Papakonstantinou C., Massuti E., Palmeri A., et al. 2011. *Notacanthus bonaparte* (Mediterranean assessment).
Piscitelli G., Matarrese A., Soriano N., et al. 1998. Osservazione sulla biologia riproduttiva di *Notacanthus bonapartei* Risso, 1840 (Teleostei, Heteromi) nel mesobatiale del mar Jonio. Biol. Mar. Medit. 5: 829–833.
Poulsen J.Y., Thorkildsen S., Arboe N.H. 2018. Identification keys to halosaurs and notacanthids (Notacanthiformes, Elopomorpha) in the subarctic Atlantic Ocean including three new distributional records and multiple molecular OTUs of *Notacanthus* cf. *chemnitzii*. Mar. Biodivers. 48: 1009–1025. https://doi.org/10.1007/s12526-017-0762-8
Priede I.G. 2017. Adaptations to the Deep Sea. In: Deep-Sea Fishes. Cambridge University Press, pp. 87–138. https://doi.org/10.1017/9781316018330.004
R Core Team. 2022. R: A language and environment for statistical computing. R Foundation for Statistical Computing. https://www.R-project.org
Romeu O.R. 2014. Biology and trophic ecology of *Notacanthus bonaparte* and *Polyacanthonotus rissoanus* (Pisces : Notacanthidae) in the Balearic Basin (Western Mediterranean). Universidad Autónoma de Barcelona.
Romeu O.R., Cartes J.E., Solé M., et al. 2016. To what extent can specialized species succeed in the deep sea? The biology and trophic ecology of deep-sea spiny eels (Notacanthidae) in the Mediterranean Sea. Deep. Res. Part I Oceanogr. Res. Pap. 115: 74–90. https://doi.org/10.1016/j.dsr.2016.05.006
Saber S., Macías D., Ortiz de Urbina J., et al. 2015. Stereological comparison of oocyte recruitment and batch fecundity estimates from paraffin and resin sections using spawning albacore (*Thunnus alalunga*) ovaries as a case study. J. Sea Res. 95: 226–238. https://doi.org/10.1016/j.seares.2014.05.003
Sangiorgi F., Quaijtaal W., Donders T.H., et al. 2021. Middle Miocene Temperature and Productivity Evolution at a Northeast Atlantic Shelf Site (IODP U1318, Porcupine Basin): Global and Regional Changes. Paleoceanogr. Paleoclimatology 36: e2020PA004059. https://doi.org/10.1029/2020PA004059
Schindelin J., Arganda-Carreras I., Frise E., et al. 2012. Fiji: an open-source platform for biological-image analysis. Nat. Methods 9: 676–682. https://doi.org/10.1038/nmeth.2019
Taslima K., Al-Emran M., Rahman M.S., et al. 2022. Impacts of heavy metals on early development, growth and reproduction of fish – A review. Toxicol. Reports 9: 858–868. https://doi.org/10.1016/j.toxrep.2022.04.013
Tesch F.W. 1968. Age and growth. In: Ricker, W.E. (ed), Methods for Assessment of Fish Production in Fresh Waters. Blackwell Scientific Publications, Oxford, UK, pp. 93– 123.

Thorsen A., Kjesbu O.S. 2001. A rapid method for estimation of oocyte size and potential fecundity in Atlantic cod using a computer-aided particle analysis system. J. Sea Res. 46: 295–308. https://doi.org/10.1016/S1385-1101(01)00090-9
Torrejon-Magallanes J. 2020. sizeMat: Estimate Size at Sexual Maturity.
Tyler C.R., Sumpter J.P. 1996. Oocyte growth and development in teleosts. Rev. Fish Biol. Fish. 6: 287–318. https://doi.org/10.1007/BF00122584
Vedishcheva E. V., Orlov A.M., Orlova S.Y., et al. 2016. First data on the age, growth processes, and otoliths of snub-nosed spiny eel *Notacanthus chemnitzii* (Notacanthidae). J. Ichthyol. 56: 890–898. https://doi.org/10.1134/S0032945216060102
Velasco F., Landa J., Barrado J., et al. 2008. Distribution, abundance, and growth of anglerfish (*Lophius piscatorius*) on the Porcupine Bank (west of Ireland). ICES J. Mar. Sci. 65: 1316–1325. https://doi.org/10.1093/icesjms/fsn130
Viñas L., Pérez-Fernandez B., Besada V., et al. 2023. PAHs and trace metals in marine surficial sediments from the Porcupine Bank (NE Atlantic): A contribution to establishing background concentrations. Sci. Total Environ. 856: 159189 https://doi.org/10.1016/j.scitotenv.2022.159189
Witthames P.R., Thorsen A., Kjesbu O.S. 2010. The fate of vitellogenic follicles in experimentally monitored Atlantic cod *Gadus morhua* (L.): Application to stock assessment. Fish. Res. 104: 27–37. https://doi.org/10.1016/j.fishres.2009.11.008